Journal of Applied Polymer Science

Chitosan from Muga silkworms (*Antheraea assamensis*) and its influence on thermal degradation behavior of poly(lactic acid) based biocomposite films

Akhilesh Kumar Pal, Ananya Das, Vimal Katiyar
Department of Chemical Engineering, Indian Institute of Technology Guwahati, Guwahati, Assam, 781039, India
Correspondence to: V. Katiyar (E-mail: vkatiyar@iitg.ernet.in)

ABSTRACT: The research work is focused on extraction of chitin from Muga silkworms (MS) and its conversion into chitosan by chemical treatment process. The extracted amount of chitin and chitosan from MS were obtained ~8 wt % and ~7 wt %, respectively. Potentiometric titrations, conductometric titrations, elemental analysis, ^{1}H-NMR and FTIR analyses were employed to calculate the degree of deacetylation of chitosan (extracted at 80 °C after 10 h) and found as 77% ± 2, 81% ± 1.8, 82% ± 2.4, 97.77% ± 0.3, and 82% ± 1.8, respectively. The deacetylation process of chitin showed pseudo-first order reaction kinetics and activation energy was estimated as ~15.5 kJ/mole. The extracted chitosan (at 80 °C after 10 h) showed higher crystallinity and improved thermal stability with respect to chitosan extracted from other marine sources. Subsequently, poly(lactic acid) (PLA) and extracted chitosan dispersed biocomposite films were prepared by solution casting method. Significant dispersion of chitosan (extracted at 80 °C after 10 h) micro-particles were observed in biocomposite films using FESEM analysis. Due to chitosan interaction with PLA, significant reduction in thermal degradation and activation energy was observed during nonisothermal degradation scan of such films using Flynn-Wall-Ozawa and Kissinger-Akahira-Sunose models. © 2016 Wiley Periodicals, Inc. J. Appl. Polym. Sci. **2016**, *133*, 43710.

KEYWORDS: biodegradable; composites; degradation; films; polysaccharides

Received 18 December 2015; accepted 28 March 2016
DOI: 10.1002/app.43710

INTRODUCTION

Chitin is a natural, inflexible and nitrogenous polysaccharide with long-chain polymer of N-acetyl glucosamine (GlcNac), which is a derivative of glucose.[1–6] Chitin is found in the exoskeletons of insects and marine creatures such as crabs, lobsters, shrimps, fungi, etc.[7–9] The arrangement of polar functional groups such as acetyl and hydroxyl groups may allow the intermolecular hydrogen bonding among adjacent polymeric chains which can further enhance the miscibility of chitin with polar polymer matrix. The preferred extraction technique of chitin can be chemical method over biological method due to cost effectiveness, lesser time consumption and higher yield. Before chemical treatment, it is necessary to remove impurities like dust, dry flesh, soluble and insoluble components. So far, the highest yield of chitin ~46 wt % was obtained from squid pens and the lowest yield ~2.3 wt % was reported from *Saccharomyces gutulata* among various other microbial sources.[3,7–9]

Deacetylation is a direct conversion step from chitin into chitosan and degree of deacetylation (DD %) suggests the possible fraction of both acetylated as well as deacetylated pendent groups on its repeat unit. Due to this, chitosan is also known as copolymer of glucosamine and acetylated glucosamine units which exhibit versatile properties like biodegradability, biocompatibility and low toxicity on the basis of its origin.[2,5,8,10–15] If the DD % of this copolymer is less than 50%, it is termed as chitin which is insoluble in most of the organic and inorganic solvents, otherwise it is entitled as chitosan which is hydrophilic in nature and soluble in weak acidic aqueous solutions such as acetic, nitric and phosphoric acids. The expansion, aggregation and stiffness of the macromolecular chains strongly depend on the DD %, whereas DD % can be regulated by tuning deacetylation reaction parameters such as temperature, reaction time, and solvent concentration.

The amine group at C-2 position in chitosan has unique properties which have raised its consumption in many applications such as packaging, agriculture, food, cosmetics, textiles, pharmaceutical, biomedical and refinement of industrial effluents.[7,16] Due to its biocompatible and biodegradable properties, it is used in cotton membranes for wound dressing which gradually wear off with time as it heals.[17] Chitin and chitosan are fungistatic in nature and hence, are compatible with lots of biologically active components used in cosmetic products. Chitosan can be used preferentially in sunscreen lotions due to covalently

linked with dyes which are capable to absorb harmful UV radiations. Chitosan and hair are owing the complementary charges which allows it to be used in shampoos, rinses, hair colorants, hair sprays, and tonics. However, consumption of chitosan supplement makes human body less likely to absorb other fat soluble vitamins like A, D, and E.[1,8,9,17–19] Chitosan has film forming ability which can be utilized in food packaging applications by mixing it with other synthetic polymers such as polyvinyl chloride (PVC) and poly(lactic acid) (PLA). PLA is biodegradable, nontoxic, and bio-based thermoplastic polyester which is hydrophobic in nature and has potential to replace some of the conventional petrochemical based polymers. It is derived from 2-hydroxy propanoic acid which is obtained from natural feedstock such as corn, sugar cane and sweet potato by different methods.[20] PLA can be used in variety of applications such as packaging, drug delivery, tissue engineering, biomedical, etc. It is noteworthy to mention that the cost of production of PLA is significantly higher than conventional polymers such as polyethylene (PE), polyethylene terephthalate (PET) and polystyrene (PS). However, the effective recycling of PLA can enhance its acceptability as commodity polymers. Therefore, more knowledge on thermal stability and recycling of such bio-based polymers are essential for its industrial viability. Thermal stability of polymers can be monitored by thermogravimetric analysis (TGA) and understanding about the degradation behaviour can be developed by thermal degradation kinetics study using various developed methods. The activation energy of polymers can be calculated using different model free methods and isoconversional methods. In this line, Carrasco *et al.*, 2010 was processed PLA by two different methods such as injection molding and extrusion followed by injection molding followed by comparing its thermal degradation kinetics with unprocessed PLA. The activation energies were found as 318 kJ/mol and 280 kJ/mol for unprocessed and processed PLA respectively using general analytical solution.[21] Mroz *et al.*, 2013 was calculated the activation energy values as 152 kJ/mol, 164 kJ/mol and 155 kJ/mol by Kissinger, Friedman, and Ozawa methods respectively for PLA films prepared by solution casting method.[22] Other researchers also calculated the activation energies of PLA prepared by different methods and found in the range of $77-171$ kJ/mol.[23,24] Thermal degradation kinetics of chitosan was also studied by many researchers and calculated the activation energy values as 149.6 kJ/mol, 138.5 kJ/mol, and 102 kJ/mol by Ozawa, Kissinger and Coats-Redfern methods.[25,26] Hence, the activation energies of PLA and chitosan cover a broad range of values as calculated by various methods.

In the present study, Muga silkworms (MS), which are found in the north eastern region (Assam) of India, were used as feedstock for synthesis of chitosan. The DD % was calculated using potentiometric titration, conductometric titration, elemental analysis, FTIR and ^{1}H-NMR analysis. ^{1}H-NMR is considered the most reliable technique for DD % calculation but potentiometric titration is the easiest and cost effective technique, compared in terms of its closeness of calculated DD % among other techniques. The temperature was fitted with DD % of chitosan using Arrhenius equation. Further, the extracted chitosan was used for preparation of PLA/Muga silkworm chitosan (PLA/MCH) based biocomposite films using solution casting method to understand the dispersion behaviour of MCH in PLA films which was observed by FESEM analysis. Influence of MCH on PLA degradation was also investigated by TGA. Activation energy and regression coefficient were calculated for all films by non-isothermal degradation kinetics with the help of Flynn-Wall-Ozawa (FWO) and Kissinger-Akahira-Sunose (KAS) models. The novelty of the present work is to investigate a new source of raw material, i.e., MS which has not been explored till now as per our literature survey. MS is dead worm or waste material which is further converted into value added products.

EXPERIMENTAL

Materials

Muga silkworm cocoons were supplied by Regional Muga Research Station, Central Silk Board, Assam, India. Cocoons were stored in a cool place before use. Hydrochloric acid, sodium hydroxide, acetone, acetic acid and sodium chloride were purchased from Sisco Research Laboratories Pvt. Ltd., India. Deuterium oxide and deutriated acetic acid were obtained from Sigma Aldrich, India. Poly(lactic acid) (2003D, granules form, density 1.24 g/cm^3) was purchased from Natureworks®, USA. All the used chemicals were of high purity and no further purification was done before analysis. Millipore water (Metrohm, ELIX 3) was used as a solvent.

Methods

Extraction of Chitin. Initially, MS were isolated from the cocoons and chopped into small pieces. The pieces were washed multiple times using normal tap water to remove dirt, dry flash and other impurities. Further, the material was dried overnight in vacuum oven at 60 °C. The dried sample was ground using mixer grinder and resulting powder was treated with 1*M* HCl solvent in a proportion of 10 mL (HCl)/g of dry powder for 20 min at 100 °C during demineralization step, as shown in Figure 1. After demineralization, the solution was filtered, thereafter, several washing with millipore water, the excess acid was removed and dried in vacuum oven till it reached to the constant weight. The demineralized MS powder was treated with 1*M* NaOH solution [10 mL (NaOH)/g of dry powder] for 24 h at 80 °C in deproteinization step. The obtained solution was appeared black in color. After filtration, the residue was washed several times with millipore water to remove excess NaOH, color, and froths. Finally, the residue was dried in vacuum oven at 60 °C to constant weight. The decoloration of deproteinized MS powder was done with acetone at room temperature for 24 h. The washed powder was filtered and dried in vacuum oven at 80 °C until constant weight. The obtained chitin powder was brown in color which was further characterized.

Deacetylation Process. In the deacetylation process, the extracted chitin sample was treated with 40% NaOH solution using chitin to solvent ratio of 1:10. The deacetylation of chitin was carried out at four different temperatures (60, 80, 100, and 110 °C) at 4, 6, 8, and 10 h for each temperature in order to understand the kinetics of the deacetylation. After deacetylation reaction, reaction mixture was washed several times with millipore water till it reached to the neutral pH $\sim$ 7. Finally, the filtered residue was dried at 60 °C in

vacuum oven until it reaches to the constant weight. The schematic flowchart of complete extraction process is shown in Figure 1.

PLA/MCH Biocomposite Films Preparation. PLA and PLA/MCH films were prepared by solution casting method. In this method, 2 g of PLA was mixed with 50 mL chloroform and a homogeneous solution was prepared by stirring it at room temperature. For the preparation of PLA/MCH biocomposite films, PLA was mixed with different MCH loading of 1, 3, and 5 wt % in chloroform followed by stirring for 6 h at room temperature. The solutions were sonicated in digital sonicator at room temperature for 2 h to reduce particle size and increase dispersion of MCH in PLA. The prepared solutions were poured on teflon petri dishes and dried for 12 h in fume hood. The films were peeled off and kept in vacuum oven at 40 °C for 12 h for further drying to remove the bound and unbound solvent completely from the films.

CHARACTERIZATION TECHNIQUES

Attenuated Total reflectance-Fourier Transform Infrared Spectroscopy (ATR-FTIR)

Infrared spectroscopic analysis was carried out for chitin and chitosan (obtained at 80 °C after 4, 6, 8 and 10 h) samples using Fourier transform infrared spectrometer (Shimazdu, IR Affinity-1) with attenuated total reflectance (ATR) attachment under dry air at room temperature. The analysis was executed in the range of 4000 cm^{-1} to 600 cm^{-1} for 20 consecutive scans at a 2.0 cm^{-1} resolution. The DD % was calculated by using eq. (1).[27]

$$DD\,\% = 97.67 - \left(26.486\frac{A_{1655}}{A_{3450}}\right) \quad (1)$$

where A_{1655} and A_{3450} are the absorbance values at wavenumber 1655 cm^{-1} and 3450 cm^{-1} respectively.

X-ray Diffractometry (XRD)

The XRD analysis of chitin and chitosan powder (obtained at 80 °C after 4, 6, 8, and 10 h) samples was performed by X-ray diffractometer (Bruker, D8 Advance, Germany). The diffractometer was equipped with Ni-filtered CuKα radiation of $\lambda = 1.54$ Å. The diverging and receiving slits were operated at 40 kV and 40 mA. The 2θ range of analysis was chosen from 3° to 40° with a continuous scan speed and increment of 2 sec/step and 0.05°/sec respectively. The samples were annealed at 60 °C for 2 h before analysis. The crystallinity index (I_{cr}) was calculated from the intensity of the peaks at $2\theta \approx 20°$ and $2\theta \approx 16°$. The peak at $2\theta \approx 20°$ showed maximum intensity which has [110] lattice plane (I_{110}) and peak at $2\theta \approx 16°$ showed minimum intensity (I_{am}), which signifies amorphous diffraction. The interlayer spacing (d) and I_{cr} were calculated by eqs. (2) and (3).[5]

$$d = \frac{\lambda}{2\sin\theta} \quad (2)$$

$$I_{cr} = \frac{I_{110} - I_{am}}{I_{110}} \times 100 \quad (3)$$

where λ is the wavelength of incident radiation. θ is half of the Bragg's angle corresponding to the crystalline peak.

Elemental Analysis

Carbon, hydrogen and nitrogen contents of extracted chitin and chitosan (obtained at 80 °C after 10 h) were measured by using CHNS Elemental Analyzer Eurovector EA3000. The sample was heated at 600 °C for 1 h and the residual weight was calculated to find out the quantity of inorganic materials. Elemental analysis was also used for estimation of DD % of chitosan samples. The eq. (4) was used to calculate the DD %.[27]

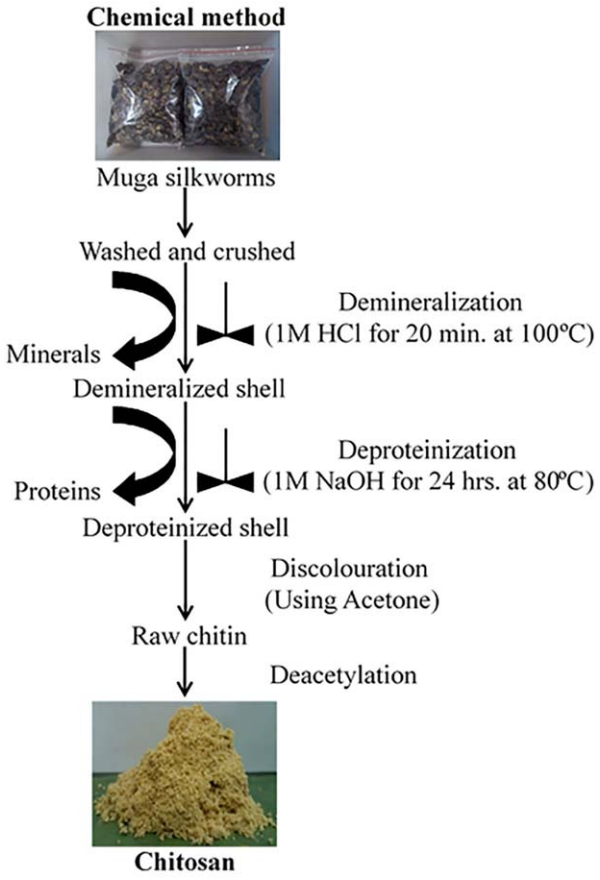

Figure 1. Schematic representation of chitosan extraction from Muga silkworms. [Color figure can be viewed in the online issue, which is available at wileyonlinelibrary.com.]

$$DD\,\% = \left(1 - \frac{\frac{C}{N} - 5.145}{6.861 - 5.145}\right) \times 100 \quad (4)$$

where $\frac{C}{N}$ is referred as carbon/nitrogen ratio of chitin and chitosan samples.

Nuclear Magnetic Resonance (^{1}H-NMR) Spectroscopy

^{1}H-NMR spectra was obtained for extracted chitosan (obtained at 80 °C after 10 h) by using Bruker Ascend^{TM}600 NMR spectrometer. The samples were prepared by dissolving 5 to 10 mg/ml of chitosan in 2% deuterated acetic acid in D_2O solution depending on the solubility of the sample. After dissolution, approximately 1 ml of chitosan sample was transferred to NMR tube for analysis. The spectra of chitosan samples were recorded in the spectral range of 0 to 10 ppm. According to ASTM F2260-03 standard, NMR spectroscopy is the most reliable characterization technique for DD calculation. Equation (5) was used for DD % calculation.[5]

$$DD\,\% = \frac{H1 - D}{H1 - D + \frac{H - Ac}{3}} \times 100 \quad (5)$$

where $H1 - D$ is the integral at $\delta = 3.17$ ppm, corresponding to the proton of the *CH* group connected to the nitrogen moiety

of the deacetylated monomer unit and $H-Ac$ is the integral at δ = 1.88 ppm, corresponding to the three protons of the acetyl group.

Potentiometric Titration

In this method, 0.2 gm of dried chitosan (obtained at 80 °C after 10 h) was dissolved in 20 ml of 0.1 M HCl solution. After 30 minutes of continuous stirring, 25 ml of millipore water was added and stirred till chitosan dissolved completely. The solution was then titrated with 0.1 M NaOH solution. The graph was plotted and two inflection points were obtained. The degree of acetylation (DA %) and DD % were calculated by the eqs. (6) and (7).[28]

$$\mathrm{DA}\,\% = 2.03\,\frac{V2-V1}{m+0.0042(V2-V1)} \tag{6}$$

$$\mathrm{DD}\,\% = 100-\mathrm{DA}\,\% \tag{7}$$

where m= dry weight of chitosan (gm), $V2-V1$ = difference in NaOH volume between the two inflection point (ml), 2.03 is the coefficient resulting from the molecular weight of chitin monomer and 0.0042 is the coefficient resulting from the difference in molecular weight between the chitin and chitosan monomer units.

Conductometric Titration

The chitosan sample (obtained at 80 °C after 10 h) was dissolved in 0.054 M HCl by stirring at room temperature and titrated with 0.165 M NaOH. The value of conductance was recorded after stabilization and plotted against the volume of titrant added. The DD % was calculated by eq. (8).[16]

$$\mathrm{DD}\,\% = \frac{[base]\times(V2-V1)\times 161}{m} \tag{8}$$

where $[base]$ is the concentration of NaOH (M), $V1$ and $V2$ are the volumes of NaOH (ml), 161 is the molar mass of the monomer and m is the amount of sample (mg).

Multistage Deacetylation Kinetics

The deacetylation of chitin to chitosan is a process that depends on the reaction temperature and time. Reactions were carried out at 60 °C, 80 °C, 100 °C and 110 °C; and the samples were collected after 4, 6, 8 and 10 h. The DD % was required for deacetylation kinetics and the values obtained by the potentiometric titration were used for the kinetic analysis. The rate of deacetylation is directly proportional to the concentration of the acetamide pendent group, hence, a pseudo-first order reaction rate eq. (9) was adopted.

$$kt = \ln\frac{a}{a-x} \tag{9}$$

where k is rate constant, a is the concentration of the original acetamide group and x is the concentration of the amine group at time t. Here, $\frac{a}{a-x}$ is proportional to (1-DD). The value of ln (1-DD) was plotted as a function of time and the value of the rate constant k was generated from the slope of plot. The linear relation ($R^2 > 0.9$) was observed between ln(1-DD) and time corresponds to the pseudo-first order reaction. Arrhenius law was used to determine the activation energy as a slope of the plot of ln(k) versus reciprocal of absolute temperature as shown in eq. (10).

$$\ln\frac{k2}{k1} = -\left(\frac{E}{R}\right)\left(\frac{1}{T2}-\frac{1}{T1}\right) \tag{10}$$

where $k1$ and $k2$ are the rate constants at temperatures $T1$ and $T2$ (K) respectively, E is the activation energy (J/mole) and R is the universal gas constant (8.314 J/mole K).[15,16,29]

Thermogravimetric Analysis (TGA)

TGA analysis was performed to examine the thermal stability of chitin and chitosan (obtained at 80 °C after 10 h) by using TGA instrument (TGA-4000, Perkin Elmer, USA). Approximately, 10 mg of sample was heated from 30 °C to 700 °C at a heating rate of 10 °C/min. under nitrogen atmosphere with a flow rate of 50 ml/min. The non-isothermal degradation kinetics for PLA/MCH biocomposite films was done in the temperature range of 30 °C to 600 °C at different heating rates from 5 °C/min to 20 °C/min.

Scanning Electron Microscopy (SEM)

SEM images of extracted chitin and chitosan (obtained at 80 °C after 10 h) samples were captured by scanning electron microscope (1430VP, LEO) with 10 kV at 15 mm working distance. All the powder samples were mounted on aluminium stubs on double sided carbon tape. The gold coating of ~ 10 nm was done by sputtering unit (SC7620, Quorum).

Viscosity Average Molecular Weight

Intrinsic viscosity [η] measurement of chitosan (extracted at 80 °C after 10 h) was performed by Ubbelohde viscometer at room temperature (25 ± 1 °C). A solvent mixture of 0.02 M acetic acid and 0.1 M sodium chloride was used to dissolve chitosan with five different concentrations from 0.001 gm/ml to 0.010 gm/ml. Intrinsic viscosity (ml/gm) was calculated using the Huggins eq. (11).[12]

$$\frac{\eta_{sp}}{C} = [\eta] + k[\eta]^2 C \tag{11}$$

where $\frac{\eta_{sp}}{C}$ is the reduced viscosity in ml/gm, η_{sp} is the relation between viscosity of the polymer in solution and the solvent (dimensionless), C is the concentration of the solution in gm/ml and k is a constant valid for each polymer (dimensionless).

The viscosity average molecular weight (M_v) of chitosan was calculated by using Mark-Houwink-Sakurada eq. (12).[12]

$$[\eta] = kM_v^{\alpha} \tag{12}$$

where $k = 1.81 \times 10^{-3}$ ml/g and $\alpha = 0.93$

The average value of three replicates was calculated for intrinsic viscosity and viscosity average molecular weight calculation.

Ash Content

Chitosan (extracted at 80 °C after 10 h) ash content was estimated through combustion process using a constant weight crucible. The empty crucible was placed in muffle furnace (Reico, India) at 600 ± 5 °C for 30 min and subsequently the residue, cooled upto room temperature, was used for weight measurement. For real time ash analysis, 1 gm of chitosan sample was treated under the identical conditions and thereafter the weight of the ash was measured followed by the calculation of ash content using eq. (13).[30]

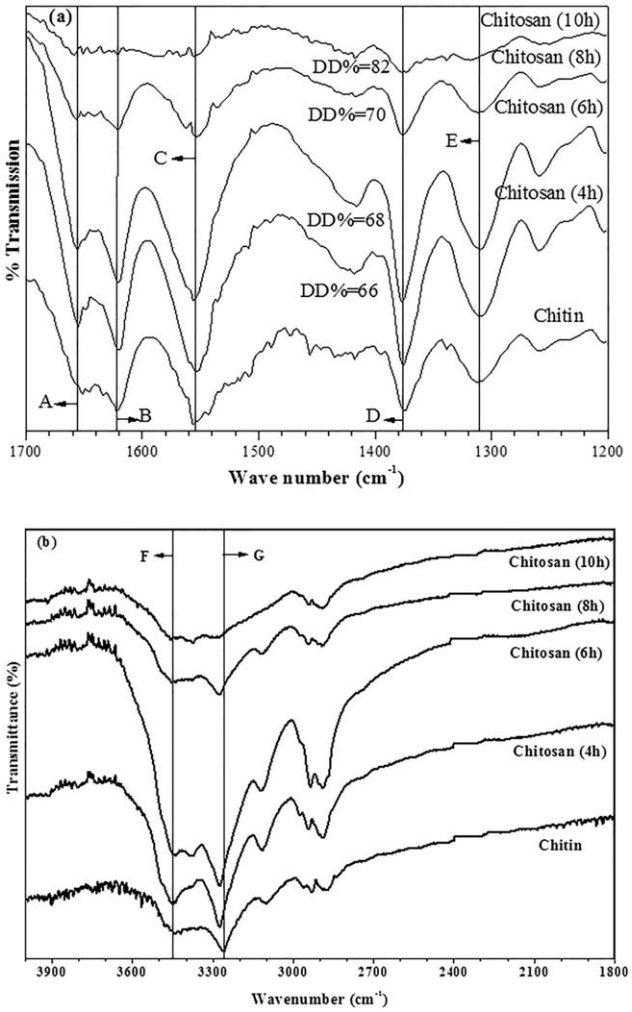

Figure 2. FTIR analysis of chitin and chitosan (a) in the range of 1200 to 1700 cm^{-1} (A = 1654-1658 cm^{-1}; B = 1620-1622 cm^{-1}; C = 1555-1557 cm^{-1}; D = 1375 cm^{-1}−1377 cm^{-1}; E = 1307-1311 cm^{-1}) and (b) in the range of 1800 to 4000 cm^{-1} (F = 3450 cm^{-1}; G = 3260 cm^{-1}−3275 cm^{-1}).

$$\text{Ash } \% = \frac{W_2 - W_0}{W_1 - W_0} \times 100 \quad (13)$$

where W_0 is the constant weight of silica crucible, W_1 is the weight of chitosan sample with crucible and W_2 is the weight of ash with crucible.

Field Emission Scanning Electron Microscopy (FESEM)

FESEM analysis of PLA and PLA/MCH biocomposite films was performed by field emission scanning electron microscope (Sigma, Zeiss). Small piece of film samples was mounted at aluminium stubs over double sided carbon tape and ~10 nm gold-palladium coating was done under vacuum by using sputter coater (SC7620, Quorum). The analysis was performed at 1.50 kV with 5.2 mm working distance.

RESULTS AND DISCUSSION

Chitin Extraction and Chitosan Conversion

The dried MS was grinded and the amount estimated as ~25 wt % of raw muga silkworm. After demineralization, the amount of dried sample was obtained ~17 wt %. The weight loss was attributed to the removal of catechols, Ca, Mg, K and other water soluble impurities. After deproteination, the amount of dried sample was estimated as ~8 wt %. The weight loss was observed due to the removal of proteinaceous elements, pigments, lipids and other organic materials. To remove color, the dried powder was mixed with acetone for 24 h however, the weight loss in this step was found negligible and the extracted dry chitin powder was found ~8 wt % on dry weight basis of raw MS. Whereas, the extracted chitosan percentage after deacetylation process was found ~7 wt % on dry weight basis of raw MS.

Attenuated Total reflectance-Fourier Transform Infrared Spectroscopy (ATR-FTIR)

In chitin sample, the absorption band at 1651 cm^{-1} shows the vibration of amide I band ($C=O$ stretching) which confirms that the extracted powder sample after discoloration is chitin as shown in Figure 2(a). The other absorption band is observed at 1557 cm^{-1} in chitin sample which shows the vibrations of amide II band ($N-H$ stretching). The associated reason is that some part of chitin may be already converted into chitosan during alkali treatment. FTIR spectra of chitosan (extracted at 80 °C) is recorded for different time (up to 10 h) interval during deacetylation process. For different chitosan samples, one band is observed in the range of 1555 cm^{-1} to 1557 cm^{-1} which denotes the vibrations of amide II band ($N-H$ stretching) and confirms that the deacetylated samples are chitosan. The vibration of amide I band at 1651 cm^{-1} in chitin sample has shifted towards higher wavenumber i.e., in the range of 1654 cm^{-1} to 1658 cm^{-1} for different deacetylated samples which indicates the more amorphous nature of chitosan samples than that of chitin. The band in the range of 1620 cm^{-1} to 1622 cm^{-1} is attributed to the stretching of $C-N$ vibration of the superimposed $C=O$ group. The absorption band at 1307 cm^{-1} to 1311 cm^{-1} corresponds to the formation of $CO-NH$ group. Whereas, the band at 1375 cm^{-1} to 1377 cm^{-1} corresponds to the symmetrical deformation of the CH_3 group in all the samples. The intensity of all above mentioned peaks is diminishing due to the deacetylation process which confirms the change in the amount of bonds in the samples. The DD % of chitosan samples are calculated by using eq. (1) and observed as 66% ± 1.5, 68% ± 1.7, 70% ± 0.9, and 82% ± 1.8 at different deacetylation time i.e., 4, 6, 8, and 10 h, respectively. The DD % value increases with increasing deacetylation time as shown in Figure 2(a). The broad absorption band at 3450 cm^{-1} corresponds to OH^{-1} group. While, the absorption band at 3260 cm^{-1} to 3275 cm^{-1} corresponds to intermolecular hydrogen bond to acetamide vibration as shown in Figure 2(b).

X-ray Diffractometry (XRD)

Crystallinity index (I_{cr}) and d-spacing of chitin and chitosan (extracted at 80 °C) were shown in Figure 3. The orthorhombic unit cells of chitin and chitosan with diffraction planes of [0,2,0], [1,1,0], and [1,0,1] were observed in line with the literature.[3,6] From the results, chitin sample shows well resolved acute reflections at 9.1° and 19.1° with minor reflections at 12.6° and 26.3° as shown in Figure 3. These sharp reflections show crystalline nature of chitin but the intensity of these reflections is low which indicates the semicrystalline nature of

chitin. Whereas, the same two peaks were observed for different deacetylated chitosans (obtained at 80 °C after 4, 6, 8 and 10 h) in the range of 2θ ≈ 9.5° to 10.2° and 2θ ≈ 19.7° to 20.05°. The observed peaks are broad, less resolved and also shift to higher 2θ values. It shows reduced crystallinity of chitin after deacetylation which concludes that chitosan has more amorphous nature than chitin. The peaks in the range of 9.1° to 10.2° represent d-spacing in the range of 8.6Å to 9.7Å due to the incorporation of bound water molecules into the crystal lattice of chitin and chitosan. The peaks in the range of 19.1° to 20.05° corresponds d-spacing in the range of 4.4Å to 4.6Å. The interlayer spacing value decreases once the chitin transform into chitosan due to the reduction in bound water molecules.

The I_{cr} value of chitin was ~84% whereas, 70-82% was observed in chitosan. The I_{cr} value for different deacetylated chitosans was different due to the penetration of alkali into the chitin crystallites. This penetration breaks the acetyl groups to modify the lattice arrangement of the chitin molecules.[27] I_{cr} also depends on DD % and decreases with increase in deacetylation time as shown in Figure 3, which shows more amorphous nature of chitosan than that of chitin. In the present work, I_{cr} for chitin was found 84% which shows the highly crystalline nature of extracted chitin from MS than that of other silkworms and insects. It is reported in the literature that chitins from larva cuticles and silkworms (*Bombyx mori*) have much lower crystallinity (only 54% and 58% respectively). The reason of low crystallinity is due to the presence of low molecular weight catechol that remains in the insect chitin.[3] Abdou *et al.*, 2008 were extracted chitin and chitosan from different marine sources and obtained percentage crystallinity is 66%, 48.9%, 43.15%, 41.78%, 40.99%, and 36.43% for brown shrimp, pink shrimp, cuttlefish pens, squid pens, crab shells, and crayfish shells, respectively.[7]

Elemental Analysis

Elemental analysis was used to measure the elemental composition (C %, H % and N %) of chitin, chitosan and DD %. The average percentage of N %, H % and C % for chitin were observed as 6.48%, 6.18%, and 42.92% respectively. Whereas, the average percentage of N %, H % and C % for chitosan (obtained at 80 °C after 10 h) were detected as 6.32%, 6.21%, and 34.42%, respectively. On comparing the elemental compositions of chitin and chitosan, it shows a small difference in N % and H % but a considerable difference in C % due to the conversion of amide group to amine group during deacetylation. So, the C % is mainly responsible for DD % and calculated as 82% ± 2.4 by eq. (4).

Nuclear Magnetic Resonance (^{1}H-NMR) Spectroscopy

The peak at 1.88 ppm indicates the three protons of the acetyl group (H-Ac) in glucosamine unit and at 3.17 ppm shows the proton of the CH group connected to nitrogen moiety of acetylated glucosamine unit (H1-D) as shown in Figure 4(a). In the spectrum of extracted chitosan (obtained at 80 °C after 10 h), all the other nonanomeric protons have peaks in the range of 3.5 to 4.0 ppm. These non-anomeric protons have similar electron densities and the peaks partially overlap each other in the given spectral range. The resolution of the other protons was low and often overlapped with the signals of the solvent (4.7 to 4.9 ppm for

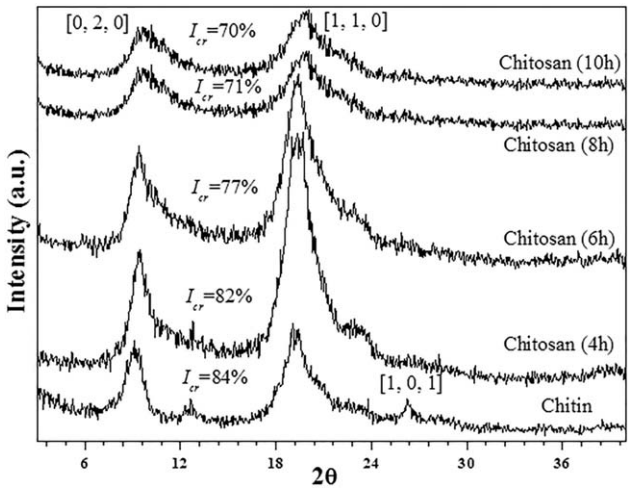

Figure 3. XRD analysis of extracted chitin and chitosan from Muga silkworms.

D_2O/2.03 ppm for CD_3COOD). The slight shift in position of the peaks may be due to the working temperature. The DD % was calculated as 97.77%±0.3 by the given formula in eq. (5).

Potentiometric Titration

The graph was plotted for pH derivative against the volume of NaOH added where two inflection points were obtained as shown in Figure 4(b). The first inflection point corresponds to the neutralization of HCl and the second to the neutralization of the ammonium ions of chitosan (obtained at 80 °C after 10 h). The difference between two inflection points gives the amount of amine groups present in chitosan. The DD % value was 77%±2 as calculated by eqs. (6) and (7).

Conductometric Titration

The conductivity graph was appeared with three distinct line segments, as shown in Figure 4(c). The first segment line corresponds to the neutralization of excess HCl present in the solution whereas second shows the neutralization of the ammonium group present in the chitosan (obtained at 80 °C after 10 h). The third segment line relate to the excess base present in the sample. The two points were found by the intersection of the three lines and the difference between the two points corresponds to the amount of NaOH required to neutralize the amine group. Using eq. (8), DD % was calculated as 81%±1.8 which was in close agreement with the values calculated by FTIR, ^{1}H-NMR, elemental analysis, and potentiometric titration.

Deacetylation Reaction Pathway

Deacetylation occurs when chitin reacts with sodium hydroxide and subsequently the carbonyl carbon gets polarized. The OH^- ions in solution attach with the carbon of amide group and form an intermediate which converts into NH^- ions and acetic acid by rearrangement of electrons. Protons from acetic acid react with NH^- ions and forms NH_2. The reaction pathway of amide to amine conversion is shown in Figure 5.

Multistage Deacetylation Kinetics

The deacetylation reaction was carried out at 60, 80, 100, and 110 °C to study the deacetylation kinetics of the process and samples were

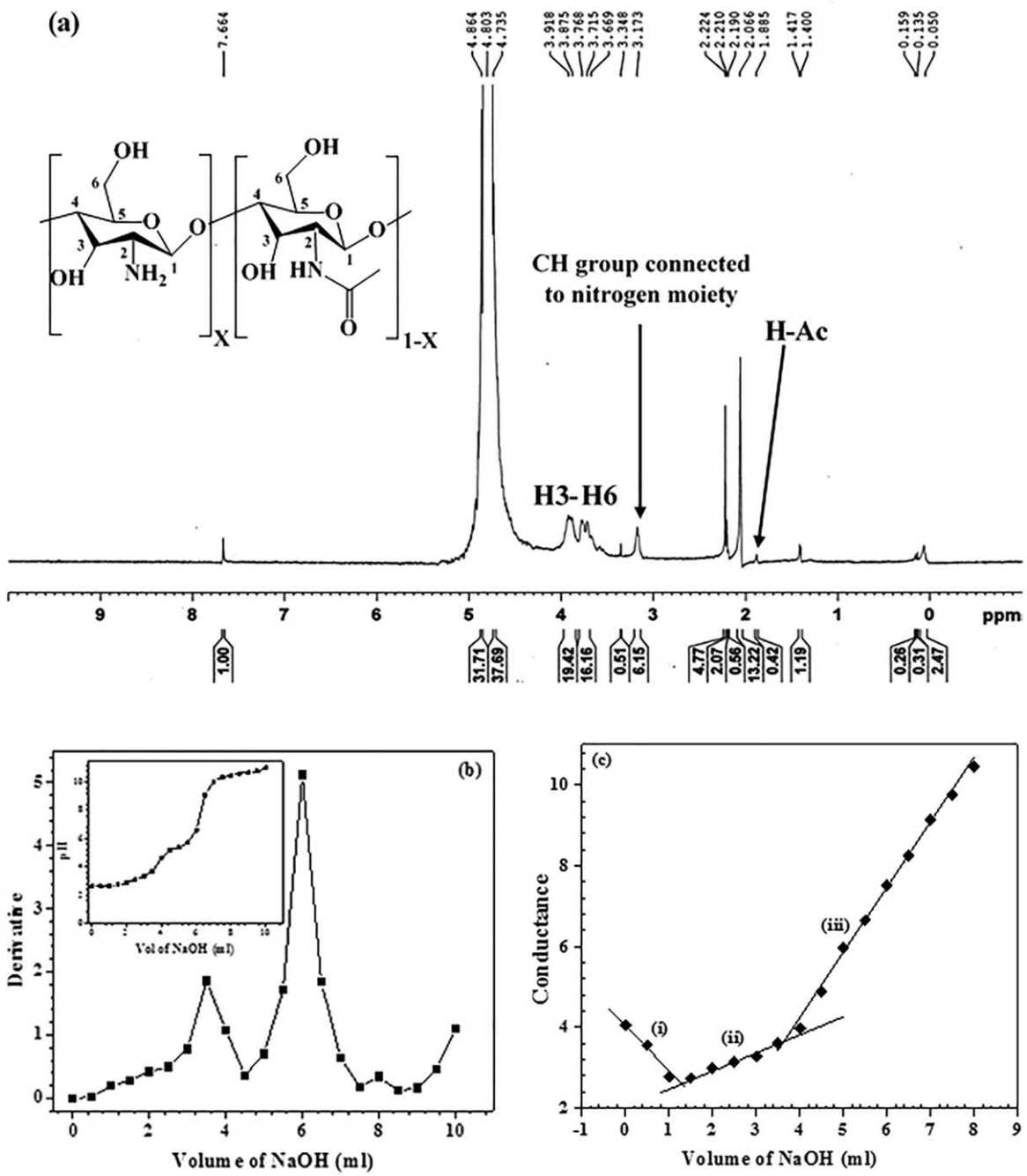

Figure 4. (a) ^{1}H-NMR of extracted chitosan; Determination of DD % by (b) Potentiometric titration and (c) Conductometric titration method.

collected after 4, 6, 8, and 10 h. The DD % of chitosan samples was calculated by potentiometric titration as shown in Table I which concludes that DD % increases with increase in deacetylation temperature, time and alkaline concentration. The conversion of chitin to chitosan was negligible at lower temperatures (<80 °C) which indicates that deacetylation process is highly temperature dependent and favorable at higher temperatures. Yaghobi *et al.*, 2010 was also found the same behavior of DD % increment with change in temperature, time and alkali concentration.[15]

The graph of –ln(1-DD) versus reaction time (t) was plotted as shown in Figure 6(a). The calculated rate constants were 0.1921 hr^{-1}, 0.287 hr^{-1} and 0.2946 hr^{-1} at 80 °C, 100 °C and 110 °C, respectively. Using Arrhenius equation [eq. (10)], the activation energy was calculated as 15.5 kJ/mol as shown in Figure 6(b). Similar results were found by some other researchers also.[15,31]

Thermogravimetric Analysis (TGA)

TGA plots of chitin and chitosan (obtained at 80 °C after 10 h) are shown in Figure 7(a). First broad peak for both chitin and chitosan was observed as endothermic peak which appeared at ~100 °C. The peak corresponds to evaporation or loss of water present in the sample because of strong affinity of water in polysaccharides which implies that they may be easily hydrated in presence of moisture. The second endothermic peak appeared in the range of 264 °C to 428 °C which corresponds to thermal degradation and decomposition of

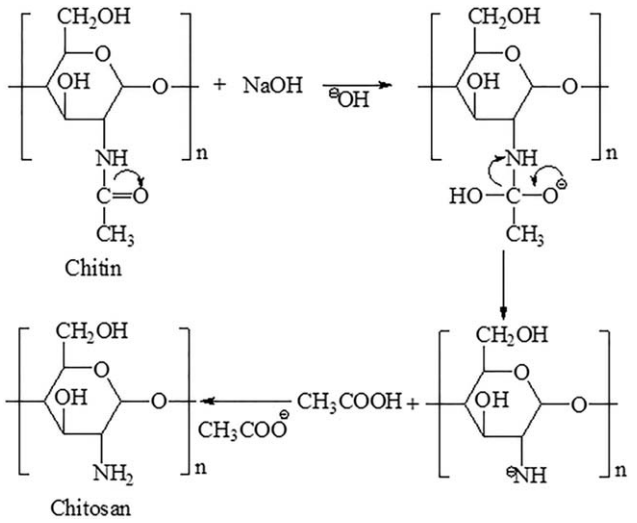

Figure 5. Reaction pathway for conversion of chitin to chitosan during deacetylation.

both the samples. The onset (T_{on}) and offset (T_{off}) temperatures for chitin and chitosan were comparable which were ~265 °C and ~428 °C, respectively. The peak temperature (T_p) of chitin (381 °C) was higher than that of chitosan (362 °C). Thermal degradation in the saccharide backbone was observed by dehydration of the saccharide rings. As observed in Figure 7(a), chitin has higher thermal stability than chitosan. Abdou *et al.*, 2008 extracted chitin and chitosan from different marine sources and found the second endothermic peak at 372 °C for chitin and 303 °C for chitosan.[7] Sagheer *et al.*, 2009 also extracted different chitins from marine sources and found the second endothermic peaks below 350 °C.[5] Hence, it confirmed that the chitin and chitosan extracted from MS have higher thermal stability than those from other sources.

Scanning Electron Microscopy (SEM)

The SEM images exhibit surface morphology of chitin and chitosan (obtained at 80 °C after 10 h) samples extracted from MS. A uniform, dense and lamellar microfibrillar crystalline structure in chitin was observed as shown in Figure 7(b). Flakes kind of structure, having rough and irregular shapes with different size, was observed in chitosan instead of microfibrils part, which confirmed more amorphous nature of chitosan than chitin as shown in Figure 7(c).[5,8,32,33]

Viscosity Average Molecular Weight

The intrinsic viscosity and viscosity average molecular weight (M_v) of extracted chitosan (obtained at 80 °C after 10 h) were calculated at room temperature (25 ± 1 °C) by Ubbelohde viscometer. Intrinsic viscosity was calculated as 37.54 mL/g by Huggins equation. The M_v of chitosan (obtained at 80 °C after 10 h) was calculated as ~44 x 10^3 Da by intrinsic viscosity values used in Mark-Houwink-Sakurada equation. Similar results were found by other researchers.[7,34–36] NaOH concentration affects chitin molecular weight during deacetylation. The higher concentration of NaOH (~70%) should not be preferred because it attacks on the backbone of chitosan. According to Ocloo *et al.*, 2011, the extracted chitosan with lower molecular weight has better antibiotic, antioxidant, antifungal, and plant growth promoting properties than that with higher molecular weight.[36]

Table I. Degree of Deacetylation at Different Temperatures Calculated by Potentiometric Titration

Deacetylation time (h)	Degree of deacetylation		
	80 °C	100 °C	110 °C
4	28 ± 1.4	31 ± 1.1	34 ± 0.7
6	43 ± 1.2	48 ± 1.4	69 ± 0.8
8	63 ± 0.9	71 ± 0.8	82 ± 1.2
10	77 ± 2	84 ± 1.6	89 ± 1.9

Ash Content

The ash content in extracted chitosan (obtained at 80 °C after 10 h) was calculated as 0.18%. The negligible amount of ash content in chitosan shows its purity. According to Liu *et al.*, 2012, the ash content of chitin and chitosan is an indication of the effectiveness of the method used for removal of inorganic materials and other impurities.[3]

Field Emission Scanning Electron Microscopy (FESEM)

In Figure 8(a), the flakes kind of structure was observed on the surface of PLA film which is completely different from PLA/MCH biocomposite films. Different size of chitosan particles were scattered in PLA matrix in PLA/MCH biocomposite films

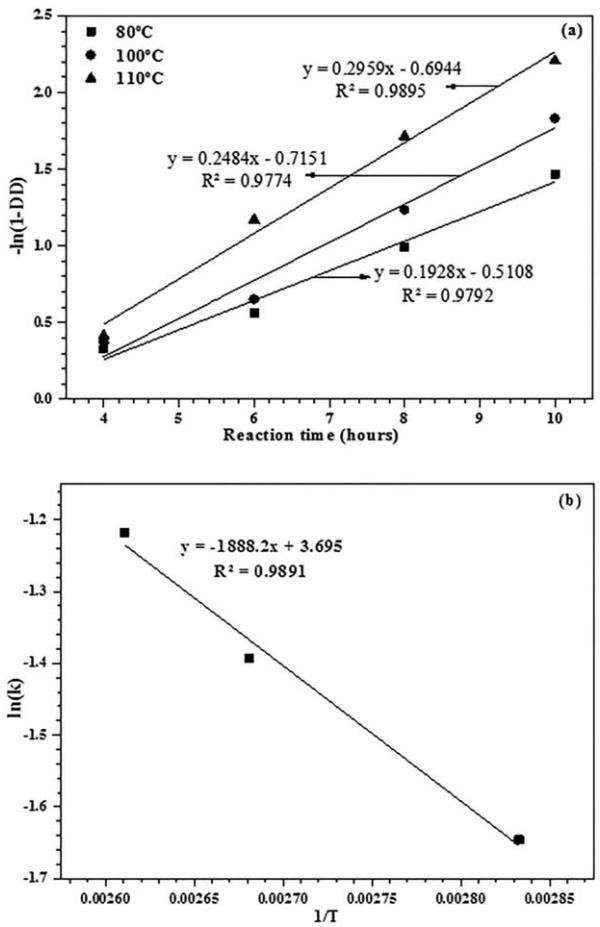

Figure 6. (a) -ln(1-DD) vs. reaction time (t) at different temperatures for potentiometric titration; (b) ln(k) vs. 1/T.

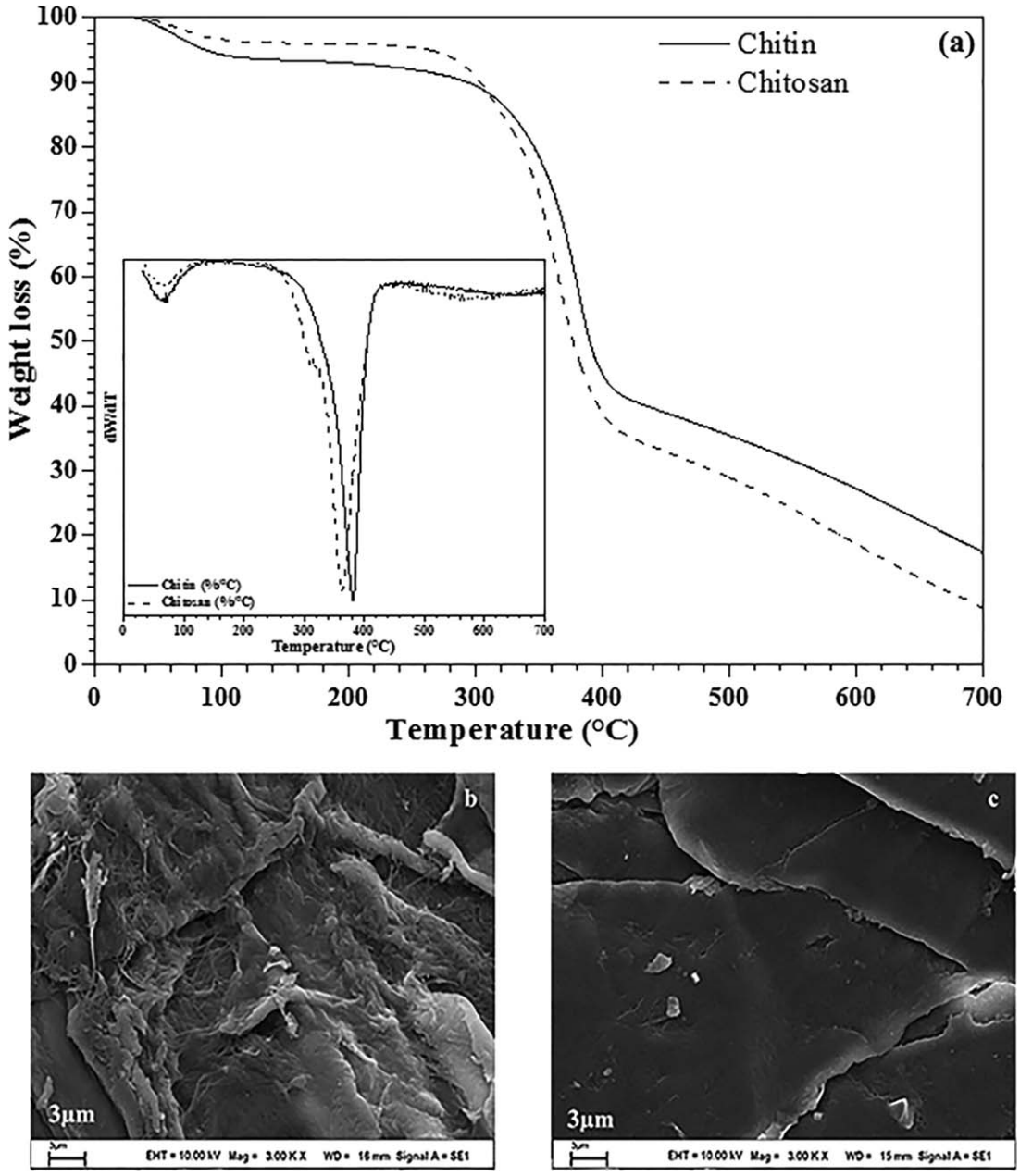

Figure 7. (a) TGA & DTG curves of chitin & chitosan; SEM images of (b) chitin and (c) chitosan.

which is clearly observed in Figure 8(b). Different size of chitosan particles were detected which were responsible for phase separation and material properties reduction. Hence, it is concluded that chitosan particles are not compatible with PLA.

Thermal Behavior of PLA/MCH Biocomposite Films

The weight % versus temperature graph with its derivative for PLA and PLA/MCH biocomposite films are shown in Figure 9 which explains the degradation behavior of all the samples at a heating rate of 20 °C/min. The two peaks with significant weight losses were observed in which the first peak was detected in the temperature range of 59 °C to 150 °C for all films that describes the release of unbound and bound moisture from the film samples. The hydrophilic nature of MCH was responsible for higher weight loss in PLA/MCH films. The maximum material degradation occurred at second peak which was in the temperature range of 345.9 °C to 394.8 °C. The thermal stability of PLA film reduced with increase in MCH concentration. The reduction in thermal stability was due to the breakage of longer polymer chains into smaller polymer chains with the addition of MCH which increased the rate of hydrolysis.

Possible reasons of PLA degradation were due to intra-molecular trans-esterification, cis-elimination and fragmentation of chains under melt state.[37,38] Whereas, the primary degradation of MCH should be due to breaking of glucosamine linkages.[39] The T_{on}, T_p, and T_{off} for PLA and PLA/MCH biocomposite films are listed in Table II.

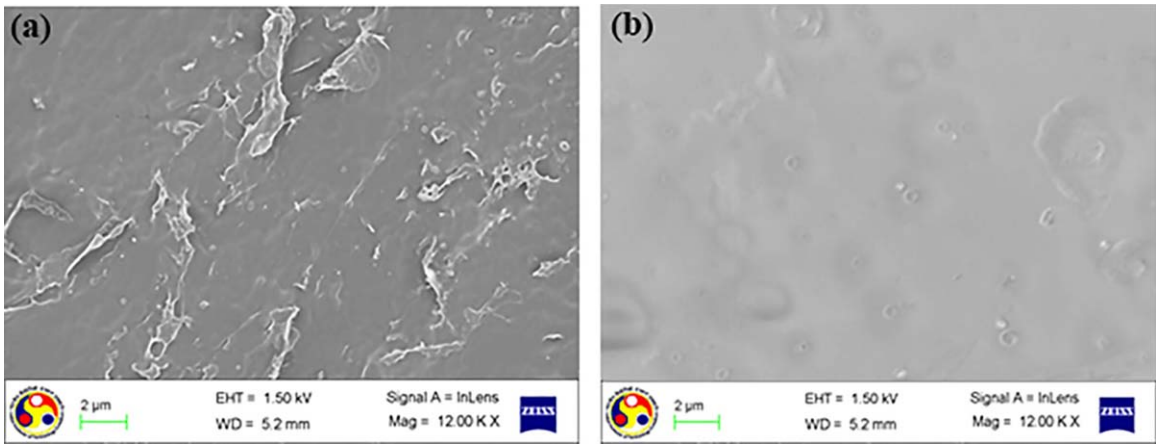

Figure 8. FESEM images of (a) PLA and (b) PLA/MCH (5%) films. [Color figure can be viewed in the online issue, which is available at wileyonlinelibrary.com.]

The TGA and DTG curves were plotted at three different heating rates of 5, 10 and 20 °C/min for each film samples as shown in Figure 10. The TGA curves were shifted to higher temperatures with increase in heating rates due to the less time provided for a sample to reach at a given temperature. The main degradation peak in all the film samples attributed to the single stage degradation.[37,38] It is because the degradation peak in the temperature range of 59 °C to 150 °C is mainly due to the moisture removal and also the change in weight % is negligible than that of degradation peak in the temperature range of 345.9 °C to 394.8 °C.

Non-Isothermal Degradation Kinetics of PLA/MCH Biocomposite Films

Thermal degradation kinetics of PLA and PLA/MCH biocomposite films were performed to develop better understanding in thermal behavior. The thermal degradation kinetics of MCH based biocomposites can be expressed by kinetic eq. (14).

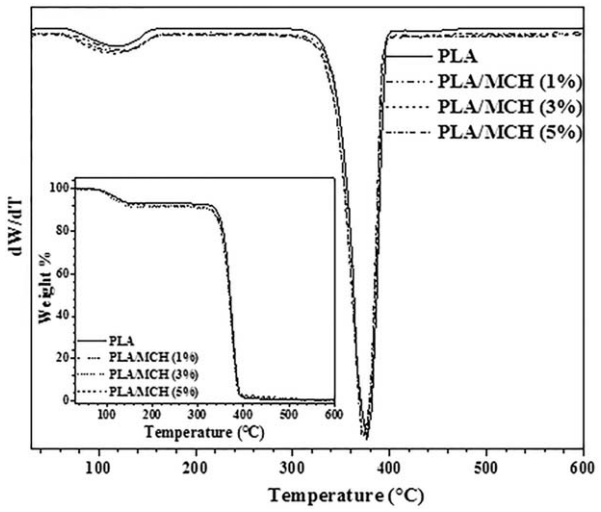

Figure 9. TGA and DTG curves of PLA and PLA/MCH biocomposite films at the heating rate of 20°C/min.

$$\frac{d\alpha}{dt} = k(T)f(\alpha) \tag{14}$$

where α, $\frac{d\alpha}{dt}$, k and $f(\alpha)$ are degree of conversion, rate of conversion, temperature rate constant and differential expression of a kinetic model function respectively.[38] The rate constant (k) can be explained by the Arrhenius equation as shown in eq. (15).

$$k(T) = A\exp\left(-\frac{E_a}{RT}\right) \tag{15}$$

where A, E_a and R are pre-exponential factor, activation energy and universal gas constant respectively. The eq. (16) can be obtained from eqs. (14) and (15).

$$\beta\frac{d\alpha}{dt} = A\exp\left(-\frac{E_a}{RT}\right)f(\alpha) \tag{16}$$

Kissinger-Akahira-Sunose Model (KAS). KAS model equation can be obtained by rearranging the eq. (16) and integrate on both sides with the initial condition of $\alpha=0$ at $T=T_0$ which gives the following expression:

$$g(\alpha) = \int_0^{\alpha}\frac{d\alpha}{f(\alpha)} = \frac{A}{\beta}\int_{T_0}^{T}\exp\left(-\frac{E_a}{RT}\right)dT \equiv \frac{AE_a}{\beta R}p\left(\frac{E_a}{RT}\right) \tag{17}$$

The Coats-Redfern approximation is the basis of KAS method which shows:

$$p\left(\frac{E_a}{RT}\right) \cong \frac{\exp\left(-\frac{E_a}{RT}\right)}{\left(\frac{E_a}{RT}\right)^2} \tag{18}$$

Table II. TGA Analysis for PLA and PLA/MCH Biocomposite Films at 20 °C/min

Sample name	Thickness (mm) ± Std. Dev.	T_{on} (°C)	T_p (°C)	T_{end} (°C)
PLA	140 ± 3	357.6	377.1	394.8
PLA/MCH (1%)	152 ± 9	356.9	375.7	392.3
PLA/MCH (3%)	162 ± 4	355.5	374.4	391.4
PLA/MCH (5%)	147 ± 9	345.9	370.2	391.2

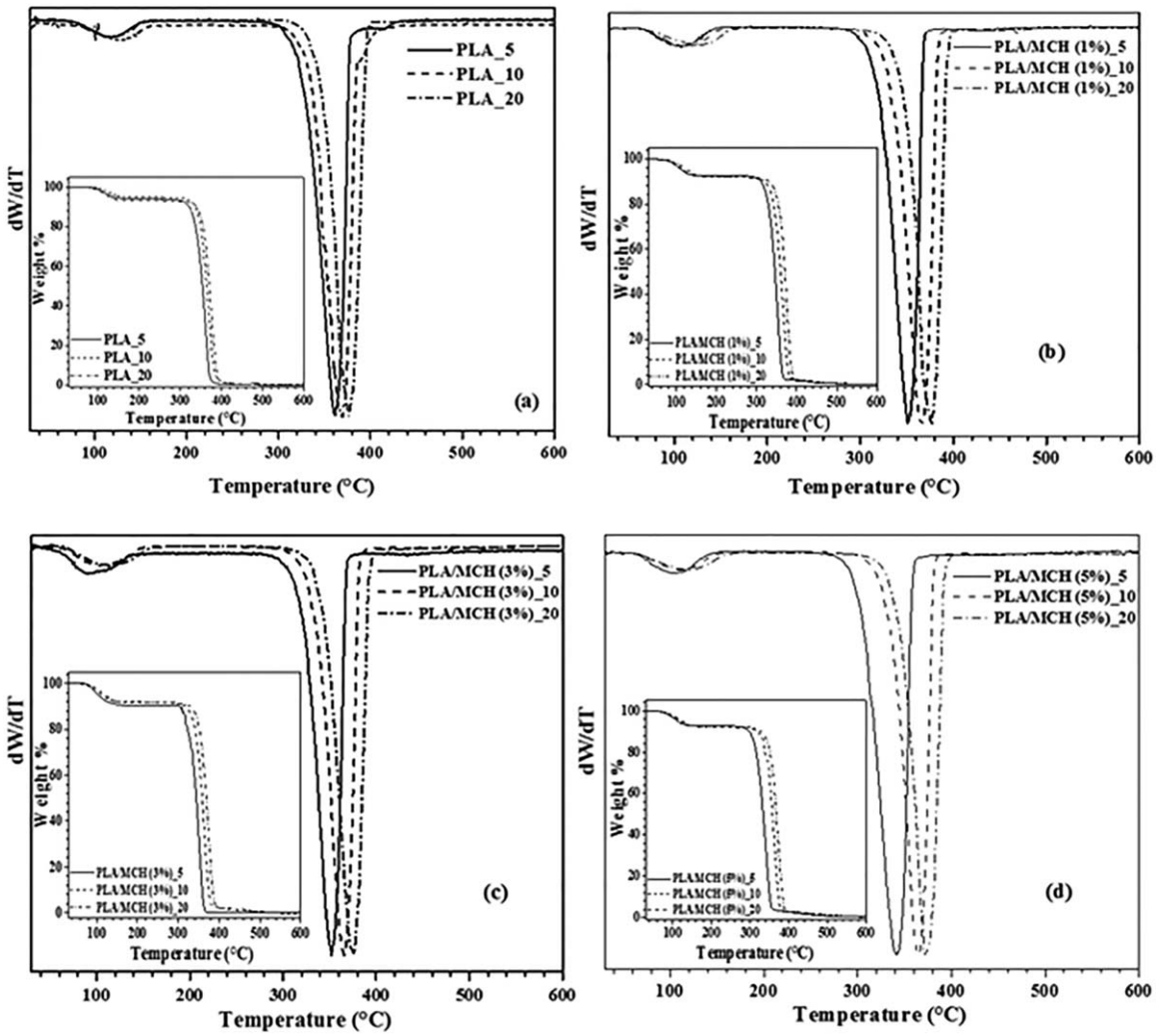

Figure 10. TGA and DTG curves of (a) PLA, (b) PLA/MCH (1%), (c) PLA/MCH (3%) and (d) PLA/MCH (5%) at the heating rates of 5, 10 and 20 °C/min.

This model is based on the assumption that A, $f(\alpha)$ and E_a are independent of temperature whereas, A and E_a are also independent of α. Equation (17) was integrated and can be written in logarithm form.

$$\ln g(\alpha) = \ln\left(\frac{AE_a}{R}\right) - \ln\beta + \ln p\left(\frac{E_a}{RT}\right) \tag{19}$$

By using eqs. (17) and (18), the final expression can be written in the form of eq. (20).

$$\ln\frac{\beta}{T^2} = \ln\left(\frac{AR}{E_a g(\alpha)}\right) - \left(\frac{E_a}{RT}\right) \tag{20}$$

The values of E_a and A can be calculated from the slope and intercept of the straight lines of $\ln\frac{\beta}{T^2}$ versus $-(\frac{1}{T})$ plot respectively.[40] KAS is based on the assumption of first order reaction model to calculate the kinetic parameters by using multiple heating rate values. The graph of $\ln\frac{\beta}{T^2}$ versus $-(\frac{1}{T})$ was plotted at different conversion values for PLA and PLA/MCH biocomposite films as shown in Figure 11. The calculated values of E_a and regression coefficients (R^2) are shown in Table III. It was concluded that the E_a values were decreased with increase in MCH concentration which confirmed the continuous reduction in thermal stability as discussed in Figure 9. The E_a values varied with the conversion which concluded that the films followed multistep degradation mechanism. The straight lines at various conversion values are nearly parallel to each other for PLA and PLA/MCH biocomposite films.

Flynn-Wall-Ozawa Model (FWO). FWO model is an integral isoconversional method which is derived by Doyle's approximation. The Doyle's approximation is expressed in the following form:

$$\ln p\left(\frac{E_a}{RT}\right) \cong -5.331 - 1.052\frac{E_a}{RT} \tag{21}$$

By using eq. (21), the eq. (19) can be rearranged as:

$$\ln\beta = \ln\left(\frac{AE_a}{g(\alpha)R}\right) - 5.331 - 1.052\frac{E_a}{RT} \tag{22}$$

The slope and intercept of the linear plot between $\ln\beta$ and $(-\frac{1}{T})$ can give the values of E_a and A.[41] Figure 12 shows the plot

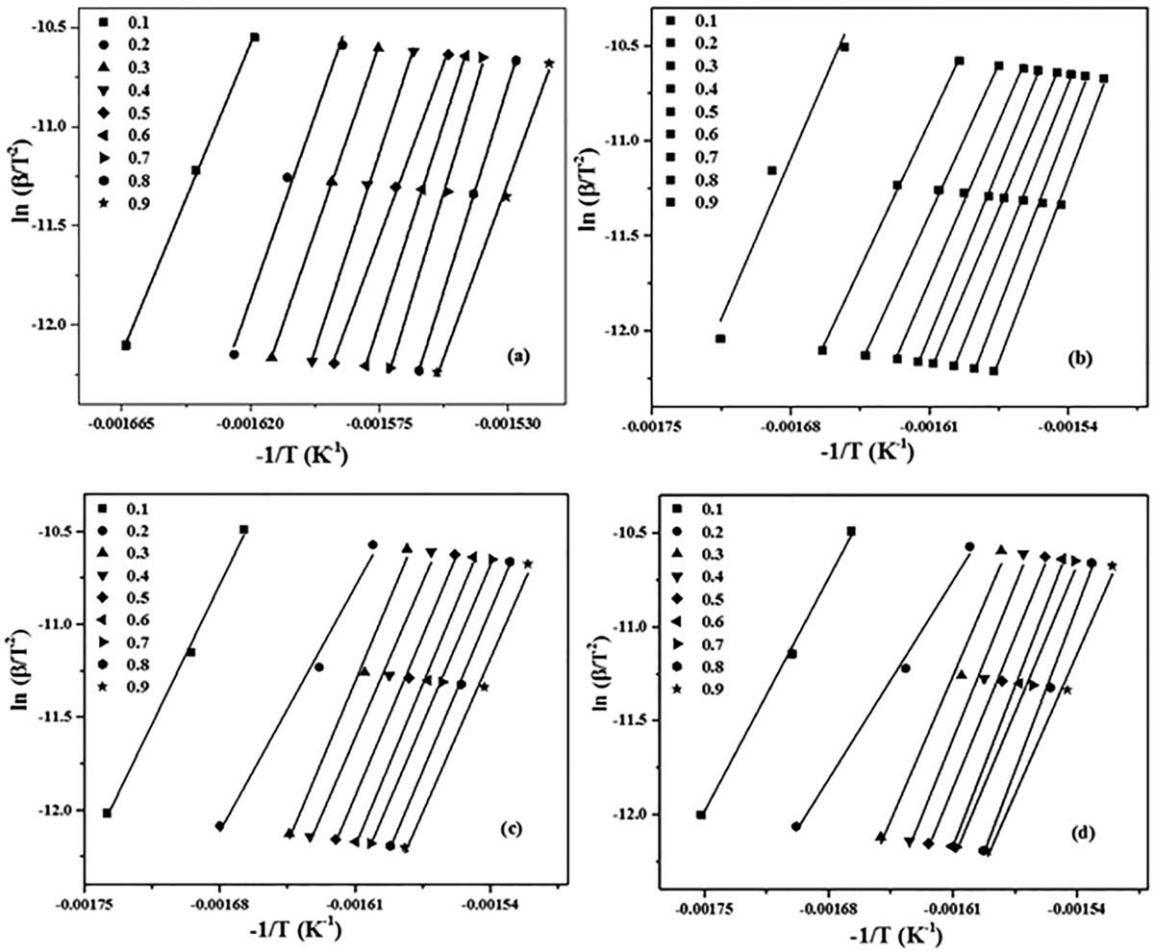

Figure 11. KAS plots of (a) PLA, (b) PLA/MCH (1%), (c) PLA/MCH (3%) and (d) PLA/MCH (5%) films.

between $\ln\beta$ and $(-\frac{1}{T})$ at different conversion values of PLA and PLA/MCH biocomposite films.

The straight lines at various conversion values are parallel to each other for the film samples which confirmed the suitability of FWO method for PLA and PLA/MCH systems. The straight lines are not completely parallel at lower α values such as 0.1 and 0.2. It shows the presence of moisture content at lower temperatures which increases with MCH content.[37,42] The E_a values follow the same pattern as in KAS method and are listed in Table III. The multistep degradation mechanism was also observed in FWO method due to variation in E_a values with conversion. The calculated E_a values from both the models were found close which showed that both isoconversional models are the best suited models for the polymeric system.

Table III. The Calculated E_a and R^2 Values from FWO and KAS Models for PLA and PLA/MCH Biocomposite Films

	KAS		FWO	
Sample Name	E_a (kJ/mol)	R^2	E_a (kJ/mol)	R^2
PLA	350.99	0.997	294.35	0.993
PLA/MCH (1%)	206.32	0.995	176.47	0.991
PLA/MCH (3%)	195.18	0.995	167.4	0.979
PLA/MCH (5%)	179.67	0.993	153.68	0.976

Activation Energy versus Conversion Plot. The calculated E_a values by FWO and KAS models were plotted in Figure 13 to observe the variation in activation energies with respect to different conversion values. The E_a values vary with increase in the degree of conversion which shows that it is purely a chemical process where no physical changes are associated with it. Basically, the change in E_a values shows a complex reaction process.[37,38] The reduction in E_a values with increase in MCH concentration showed the presence of higher acidic sites available during thermal degradation in PLA matrix. The acidic sites accelerates the auto-catalytic effect during degradation of PLA. In the case of PLA/MCH biocomposite films, the chitosan was converted into anhydrous chitosan by the removal of moisture during thermal degradation which is responsible for generation and increment of H^+ ions. H^+ ions increased with increase in MCH concentration which highly supports the degradation process of biocomposite films.

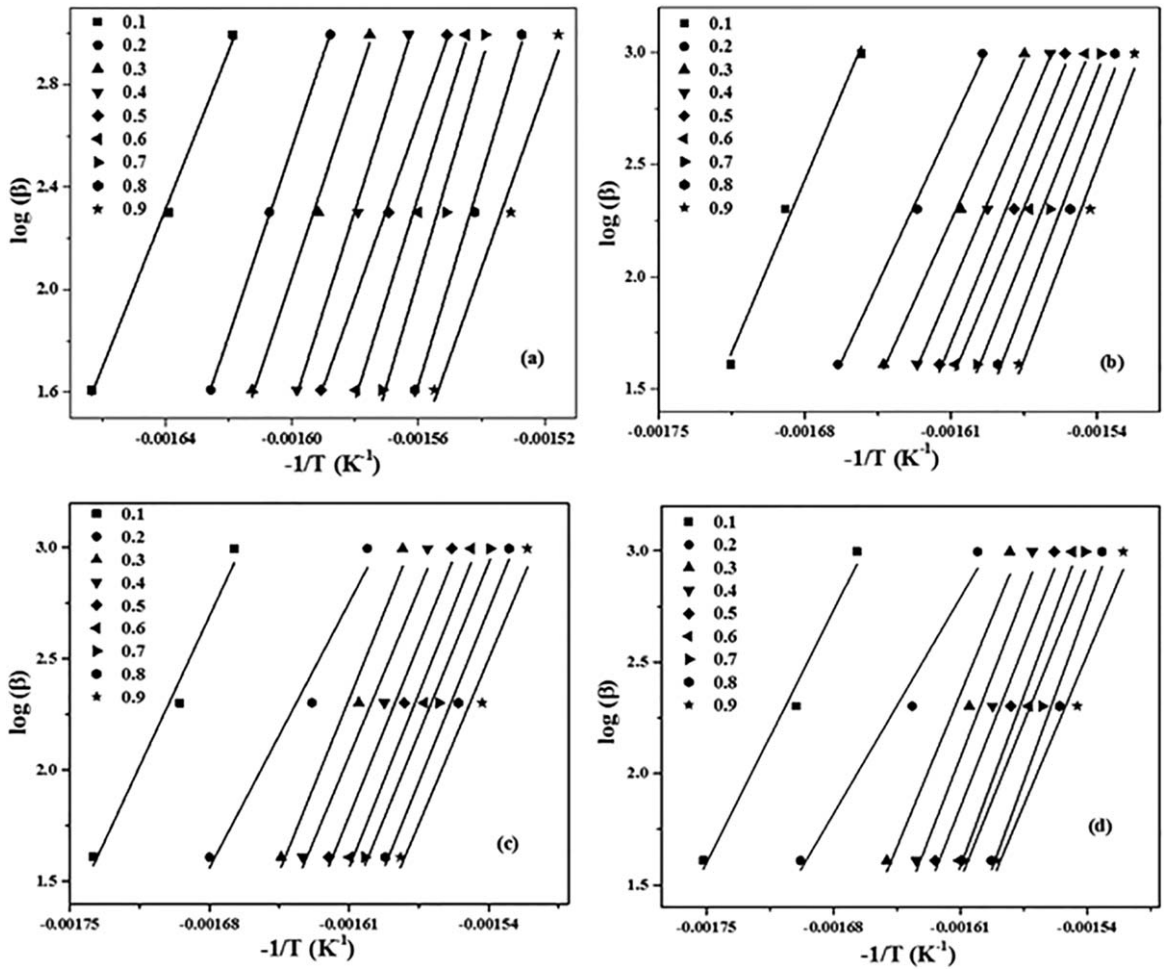

Figure 12. FWO plots of (a) PLA, (b) PLA/MCH (1%), (c) PLA/MCH (3%) and (d) PLA/MCH (5%) biocomposite films.

CONCLUSIONS

Chitin was sucessfully extracted from muga silkworms and subsequently its transformation into chitosan by deacetylation. The yield of extracted chitosan was 7% (dry weight basis) of raw MS. Different values of DD % was calculated as 77% ± 2, 81% ± 1.8, 82% ± 2.4, 97.77% ± 0.3, and 82% ± 1.8 using various methods. Activation energy for deacetylation process was found to be 15.5 kJ/mole. Crystallinity index calculated for extracted chitin and chitosan was 84% and 70% respectively. The degradation temperature for the extracted chitin and chitosan was 381 °C and 362 °C respectively which showed higher thermal stability than that of reported values in literature.

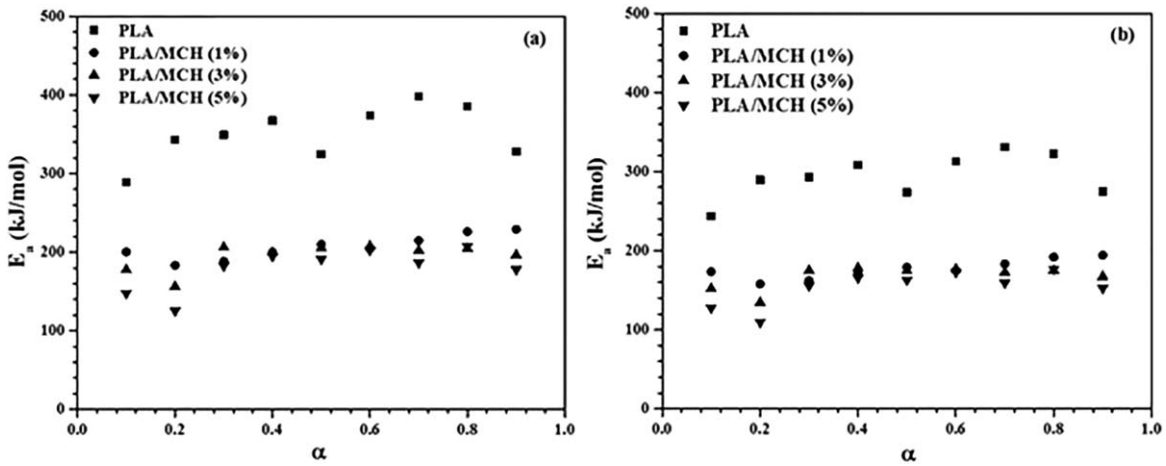

Figure 13. Activation energy vs conversion plot for (a) KAS model and (b) FWO model.

Intrinsic viscosity and viscosity average molecular weight of chitosan were calculated as 37.5 ml/gm and 44 × 10^3 Da respectively. In solution casted PLA/MCH biocomposite films, the phase separation between PLA and chitosan may result the reduction in characteristic properties. The calculated activation energies from KAS and FWO models reduced with increase in MCH loading. Both isoconversional models are suitable for such polymeric system due to values of regression coefficients close to 1. This report explores an inexpensive waste material for extraction of value added chitosan which is having diverse application in the field of pharmaceuticals, cosmetics and food.

ACKNOWLEDGMENTS

Authors are thankful to Department of Chemical and Petrochemical (DCPC), Govt. of India funded Centre of Excellence for Sustainable Polymers (CoE-SusPol), Ministry of Food Processing Industries (GoI) for reseach grant for 'GreenPack' project, Central Instruments Facility (CIF) and Department of Chemical Engineering, Indian Institute of Technology, Guwahati, India for providing research and analytical facilities.

REFERENCES

1. George, T. S.; Guru, K. S. S.; Vasanthi, N. S.; Kannan, K. P. *World J. Sci. Technol.* **2011**, *1*, 43.
2. Jiang, T.; Deng, M.; James, R.; Nair, L. S.; Laurencin, C. T. *Acta Biomaterialia* **2014**, *10*, 1632.
3. Liu, S.; Sun, J.; Yu, L.; Zhang, C.; Bi, J.; Zhu, F.; Qu, M.; Jiang, C.; Yang, Q. *Molecules* **2012**, *17*, 4604.
4. Mohammed, M. H.; Williams, P. A.; Tverezovskaya, O. *Food Hydrocoll.* **2013**, *31*, 166.
5. Sagheer, F. A. A.; Al-Sughayer, M. A.; Muslim, S.; Elsabee, M. Z. *Carbohydr. Polym.* **2009**, *77*, 410.
6. Zhang, M.; Haga, A.; Sekiguchi, H.; Hirano, S. *Biol. Macromol.* **2000**, *27*, 99.
7. Abdou, E. S.; Nagy, K. S. A.; Elsabee, M. Z. *Bioresource Technol.* **2008**, *99*, 1359.
8. Paulino, A. T.; Simionato, J. I.; Garcia, J. C.; Nozaki, J. *Carbohydr. Polym.* **2006**, *64*, 98.
9. Synowiecki, J.; Al-Khateeb, N. A. *Crit. Rev. Food. Sci. Nutr.* **2003**, *43*, 145.
10. Galed, G.; Miralles, B.; Panos, I.; Santiago, A.; Heras, A. *Carbohydr. Polym.* **2005**, *62*, 316.
11. Liu, T. G.; Li, B.; Huang, W.; Lv, B.; Chen, J.; Zhang, J. X.; Zhu, L. P. *Carbohydr. Polym.* **2009**, *77*, 110.
12. Moura, C. M. D.; Moura, J. M. D.; Soares, N. M.; De Almeida Pinto, L. A. *Chem. Eng. Proc. Process Intens.* **2011**, *50*, 351.
13. Phongying, S.; Aiba, S.; Chirachanchai, S. *Polymer* **2007**, *48*, 393.
14. Watthanaphanit, A.; Susaphol, P.; Tamura, H.; Tokura, S.; Rujiravanit, R. *Carbohydr. Polym.* **2010**, *79*, 738.
15. Yaghobi, N.; Hormozi, F. *Carbohydr. Polym.* **2010**, *81*, 892.
16. Alvarenga, E. S. D.; Pereira de Oliveira, C.; Bellato, C. R. *Carbohydr. Polym.* **2010**, *80*, 1155.
17. Dutta, P. K.; Dutta, J.; Tripathi, V. S. *J. Sci. Indus. Res.* **2004**, *63*, 20.
18. Kannan, M.; Nesakumari, M.; Rajarathinam, K.; Ranjit Singh, A. J. A. *Adv. Biol. Res.* **2010**, *4*, 10.
19. Rinaudo, M. *Prog. Polym. Sci.* **2006**, *31*, 603.
20. Rasal, R. M.; Janorkar, A. V.; Hirt, D. E. *Prog. Polym. Sci.* **2010**, *35*, 338.
21. Carrasco, F.; Pages, P.; Gamez-Perez, J.; Santana, O. O.; Maspoch, M. L. *Polym. Degrad. Stabil.* **2010**, *95*, 2508.
22. Mroz, P.; Bialas, S.; Mucha, M.; Kaczmarek, H. *Thermochim. Acta* **2013**, *573*, 186.
23. Tsuji, H.; Fukui, I. *Polymer* **2003**, *44*, 2891.
24. Carrasco, F.; Perez-Maqueda, L. A.; Santana, O. O.; Maspoch, M. L. I. *Polym. Degrad. Stabil.* **2014**, *101*, 52.
25. Britto, D. D.; Campana-Filho, S. P. *Thermochim. Acta* **2007**, *465*, 73.
26. Georgieva, V.; Zvezdova, D.; Vlaev, L. *Chem. Central J.* **2012**, *6*, 81.
27. Baskar, D.; Sampath Kumar, T. S. *Carbohydr. Polym.* **2009**, *78*, 767.
28. Czechowska-Biskup, R.; Jarosinska, D.; Rokita, B.; Ulanski, P.; Rosiak, J. M. *Prog. Chem. Appl. Chitin Its Derivatives* **2012**, *XVII*, 5.
29. Kasaai, M. R. *Carbohydr. Polym.* **2010**, *79*, 801.
30. Yuan, Y.; Chesnutt, B. M.; Haggard, W. O.; Bumgardner, J. D. *Materials* **2011**, *4*, 1399.
31. Tolaimate, A.; Desbrieres, J.; Rhazi, M.; Alagui, A.; Vincendon, M.; Vottero, P. *Polymer* **2000**, *41*, 2463.
32. Ramasamy, P.; Subhapradha, N.; Shanmugam, V.; Shanmugam, A. *Int. J. Biol. Macromol.* **2014**, *64*, 202.
33. Zhang, Y.; Xue, C.; Li, Z.; Zhang, Y.; Fu, X. *Carbohydr. Polym.* **2006**, *65*, 229.
34. Abdel-Fattah, W. I.; Jiang, T.; El-Tabie El-Bassyouni, G.; Laurencin, C. T. *Acta Biomaterialia* **2007**, *3*, 503.
35. Kasaai, M. R.; Arul, J.; Charlet, G. N. *J. Polym. Sci. Part B: Polym. Phys.* **2000**, *38*, 2501.
36. Ocloo, F. C. K.; Quayson, E. T.; Adu-Gyamfi, A.; Quarcoo, E. A.; Asare, D.; Serfor-Armah, Y.; Woode, B. K. *Radiat. Phys. Chem.* **2011**, *80*, 837.
37. Valapa, R.; Pugazhenthi, G.; Katiyar, V. *Int. J. Biol. Macromol.* **2014**, *65*, 275.
38. Pal, A. K.; Katiyar, V. *Asian Chitin J.* **2015**, *11*, 37.
39. Bonilla, J.; Fortunati, E.; Vargas, M.; Chiralt, A.; Kenny, J. M. *J. Food Eng.* **2013**, *119*, 236.
40. Aboulkas, A.; El harfi, K.; El bouadili, A. *Energy Conversion Manage.* **2010**, *51*, 1363.
41. Ou, C. Y.; Zhang, C. H.; Li, S. D.; Yang, L.; Dong, J. J.; Mo, X. L.; Zeng, M. T. *Carbohydr. Polym.* **2010**, *82*, 1284.
42. Marquez, Y.; Franco, L.; Puiggali, J. *Thermochim. Acta* **2012**, *550*, 65.

SGML and CITI Use Only
DO NOT PRINT